Available online at www.sciencedirect.com
SCIENCE DIRECT
Aquaculture 256 (2006) 272–286
Aquaculture
www.elsevier.com/locate/aqua-online

Remote estimation of chlorophyll concentration in hyper-eutrophic aquatic systems: Model tuning and accuracy optimization

Paul V. Zimba [a,*], Anatoly Gitelson [b]

[a] United States Department of Agriculture, Agricultural Research Service, Catfish Genetics Research Unit, Post Office Box 38, Stoneville, MS 38776, USA
[b] Center for Advanced Land Management Information Technologies (CALMIT), School of Natural Resources, University of Nebraska-Lincoln, Lincoln, NE 68588-0517, USA

Received 12 October 2005; received in revised form 24 January 2006; accepted 10 February 2006

Abstract

Accurate assessment of phytoplankton chlorophyll *a* (chl *a*) concentration by remote sensing is challenging in turbid hyper-eutrophic waters. This paper assessed methods to resolve this problem. A hand-held spectroradiometer was used to measure subsurface spectral reflectance (R) in the visible and near infrared range of the spectrum. Water samples were collected concurrently and contained variable chlorophyll *a* concentration (chl *a* from 107 to more than 3000 mg/m^3) and turbidity (from 11 to 423 NTU) levels. The conceptual three-band model $[R^{-1}(\lambda_1)-R^{-1}(\lambda_2)]\times R(\lambda_3)$ and its special case, the two-band model $R(\lambda_3)/R(\lambda_1)$, were spectrally tuned in accord with optical properties of the media to optimize spectral bands (λ_1, λ_2 and λ_3) for accurate chlorophyll *a* estimation. Strong linear relationships were established between analytically measured chl *a* and both the three-band $[R^{-1}(650)-R^{-1}(710)]\times R(740)$ and the reflectance ratio model $R(714)/R(650)$. The three-band model accounted for 7% more variation of chl *a* concentration than the ratio model (78 vs. 71%). Assessment of the model accuracy in dense algal blooms is hampered by the spatial and temporal inhomogeneity of algal distributions—in these waters, non-random algal distributions accounted for more than 20% spatial and up to 8% temporal variation in chlorophyll *a* concentration. The findings underlined the rationale behind the conceptual model and demonstrated the robustness of the algorithm for chl *a* retrieval in very turbid, hyper-eutrophic waters.
Published by Elsevier B.V.

Keywords: Aquaculture; Channel catfish; Chlorophyll; Cyanobacteria; Remote sensing; Turbidity

1. Introduction

Rapid assessment of water quality will become more critical as competing needs for water intensify. With more than 50% of the world's population located along coastal watersheds and large lakes (Vitousek et al., 1997) competing water uses, including potable water requirements, irrigation needs for agriculture and attempts to minimize estuarine water flow reductions, can be difficult to resolve. Uncontrolled water use coupled with drought can have dramatic negative impacts on ecosystem function such as occurred, for example, in the Murray-Darling Rivers, Australia (e.g., Australian Government Department of the Environment and Heritage website http://www.deh.gov.au/water/rivers/nrhp/), and illustrate the need for rapid, accurate assessment of aquatic ecosystem health.

* Corresponding author.
E-mail address: pzimba@msa-stoneville.ars.usda.gov (P.V. Zimba).

0044-8486/$ - see front matter. Published by Elsevier B.V.
doi:10.1016/j.aquaculture.2006.02.038

One effective method for synoptic monitoring of ecosystem health is remote sensing. Even a few images are useful as aids in the design or improvement of point sampling programs, often through highlighting the best locations and timing for sampling. Remote sensing studies typically involve the mapping of concentrations of a given variable in water bodies using radiance or reflectance collected by a sensor placed above the water surface. Estimation of concentration usually requires the development of empirical or semi-empirical models correlating upwelling radiance (or reflectance) measured remotely, and so-called "ground-truth" data (i.e., concentration of constituents of interest). Historically remote sensing of chlorophyll *a* (chl *a*) concentration was confined to open ocean case 1 waters (Morel and Prieur, 1977) using the blue and the green spectral regions (e.g., Gordon and Morel, 1983). Attempts to apply case 1-derived algorithms to case 2 productive waters (Morel and Prieur, 1977), containing widely variable and poorly correlated chl *a*, suspended solids and dissolved matter concentrations resulted in poor predictive ability (e.g., GKSS, 1986; Dall'Olmo et al., 2005). Absorption in the blue spectral region by dissolved organic matter, tripton and phytoplankton pigments is high, requiring the use of other spectral regions for chl *a* estimation.

In several cases, fluorescence line height has been used successfully for the remote detection of chl *a* in case 2 waters (Neville and Gower, 1977; Gower, 1980; Doerffer, 1981; GKSS, 1986; Fischer and Kronfeld, 1990; Gower et al., 1999). However, quantitative accuracy is limited by the varying fluorescence efficiency of different phytoplankton populations and by changes in water absorption that reduce the available light for fluorescence. While this technique seems to be useful for chl *a* assessment, generalizations and comparisons based on previous studies are very difficult to make, especially for productive turbid waters with highly variable optical properties.

The spectral features of productive waters have been studied for a wide range of chl *a* concentrations from 3 to more than 180 mg/m^3 (Gitelson et al., 1986, 1993a,b, 1994a, 2000; Millie et al., 1995; Gitelson and Kondratyev, 1991; Gitelson, 1992; Dekker, 1993; Quibell, 1992; Matthews and Boxall, 1994; Gons, 1999, 2000; Zimba and Thomson, 2002). The main spectral features of reflectance found in such waters were a trough at 670 nm and a peak around 700 nm. This peak is in the spectral range of minimal combined absorption of algae, inorganic suspended matter, dissolved organic matter and water, and is shifted toward longer wavelengths as chl *a* concentration increases (Gitelson et al., 1986; Vos et al., 1986; Gitelson, 1992, 1993; Matthews and Boxall, 1994). The magnitude of this peak was found to be related to chl *a* concentration, but was also affected by other factors including backscattering and absorption by other constituents.

To quantify chl *a*, a variety of different algorithms have been developed; all are based on the properties of the peak near 700 nm. These include the ratio of reflectance of the peak (R_{max}) to the reflectance at 670 nm (R_{670}), R_{max}/R_{670} or the ratio R_{705}/R_{670} (Gitelson et al., 1986, 1993a,b; Gitelson and Kondratyev, 1991; Dekker, 1993) and the position of this peak (Gitelson, 1992). Gons (1999) used the reflectance ratio at 704 and 672 nm and absorption and backscattering coefficients at these wavelengths to assess chl *a* concentrations ranging from 3 to 185 mg/m^3. Alternatively, good correlations have been found between chl *a* and band ratios consisting of a band at 675 nm in the denominator and one beyond 725 nm in the numerator (Hoge et al., 1987; Yacobi et al., 1995; Pierson and Sträombäack, 2000; Ruddick et al., 2001; Pulliainen et al., 2001; Oki and Yasuoka, 2002; Dall'Olmo and Gitelson, 2005).

These methods are based on the assumption that optical parameters such as the chl *a* specific absorption coefficient, $a^*_{chl\ a}(\lambda)$, and the chl *a* fluorescence quantum yield, η, remain constant. In reality, these parameters depend on the physiological state and structure of the phytoplankton community and can vary widely. Bricaud et al. (1995) showed that $a^*_{chl\ a}(675)$ can vary up to fourfold for chl *a* ranging between 0.02 and 25 mg m^{-3}. Fluorescence quantum yield is affected by phytoplankton taxonomic composition, illumination conditions, light adaptation, nutritional status and temperature, and can vary by eightfold (e.g., GKSS, 1986). Therefore, the assumptions of constant $a^*_{chl\ a}$ and η can be a significant source of uncertainty in models for remote chl *a* estimation.

Recently, a conceptual model was developed and used for estimating pigment concentration of terrestrial vegetation (Gitelson et al., 2003a; Gitelson et al., 2005):

$$\text{Pigment concentration} \propto [R^{-1}(\lambda_1) - R^{-1}(\lambda_2)] \times R(\lambda_3) \quad (1)$$

Where $R(\lambda_1)$, $R(\lambda_2)$ and $R(\lambda_3)$ are reflectances at wavelengths λ_1, λ_2 and λ_3, respectively. λ_1 is a spectral region such that $R(\lambda_1)$ is maximally sensitive to the absorption by the pigment of interest, although it is still affected by the absorption of other pigments and scattering by all particular matters. λ_2 is a spectral region such that $R(\lambda_2)$ is minimally sensitive to the absorption by the pigment of interest, and maximally sensitive to the absorption by other constituents. It was assumed that the absorption by other constituents at λ_2 was close to that at λ_1. Thus, the difference $[R^{-1}(\lambda_1) - R^{-1}(\lambda_2)]$ is related to

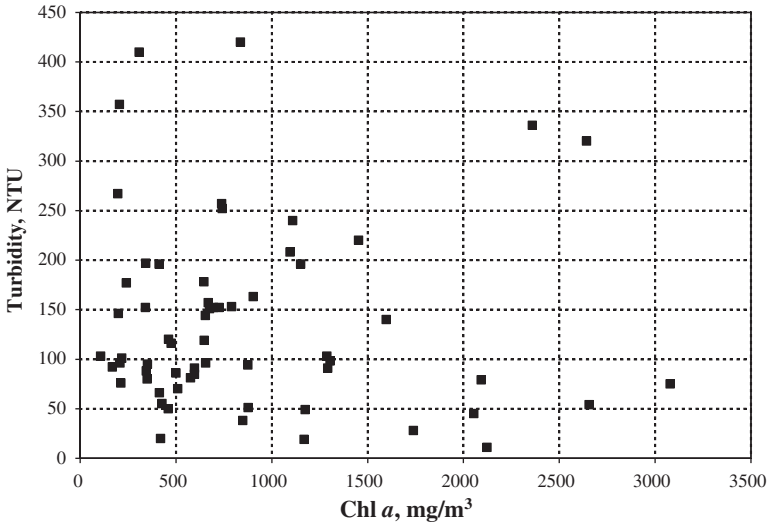

Fig. 1. Chlorophyll *a* concentration vs. turbidity in sampled ponds. Determination coefficient for linear relationship (r^2)<0.005. Chlorophyll *a* and turbidity are practically independent, indicating these ponds belong to case 2 waters.

the concentration of a pigment of interest. However, it was still affected by the variability in scattering by the medium (Gitelson et al., 2003a; Dall'Olmo and Gitelson, 2005). λ_3 is a spectral region where reflectance is minimally affected by the absorption of pigments and is therefore used to account for the variability in scattering between samples.

This conceptual model has been applied for chl *a* assessment in turbid productive waters; with model tuning in accordance with optical properties of the medium, the optimal locations of spectral bands were found (Dall'Olmo et al., 2003). Dall'Olmo and Gitelson (2005, in press) demonstrated how the spectral locations of the bands (λ_1, λ_2 and λ_3) used affected the accuracy of chl *a* estimation. Specific spectral regions where the accuracy of the algorithm is maximally affected by interferences due to the variability in bio-optical parameters of the medium and uncertainties in reflectance measurements have been found. As these bio-optical parameters, such as $a^*_{\mathrm{chl}\ a}(\lambda)$, η, are typically not determined, it would be impossible to parameterize the model. To improve the accuracy of chl *a* estimation, Dall'Olmo and Gitelson (2005) proposed to tune the band positions of the model minimizing these effects. The results of the spectral tuning of the model and the calibration coefficients obtained depend on optical

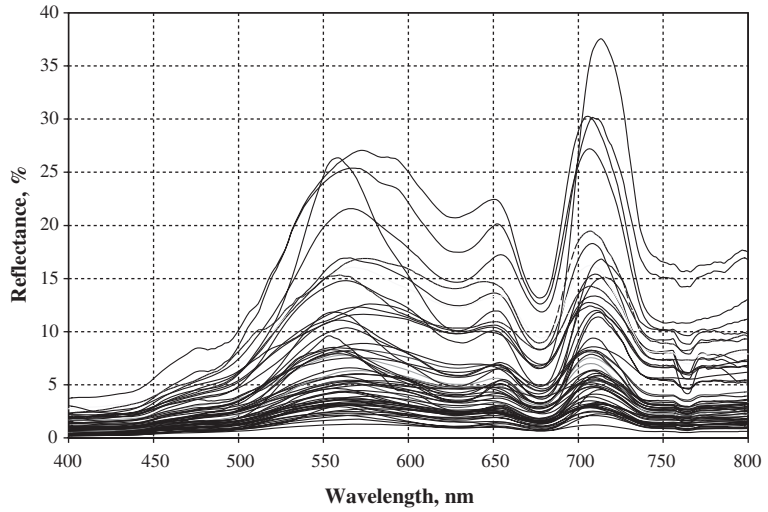

Fig. 2. Reflectance spectra of aquaculture ponds studied.

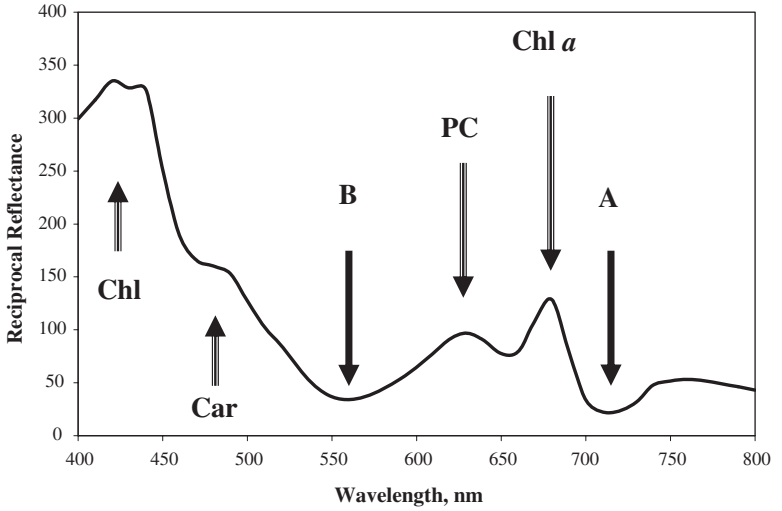

Fig. 3. Typical reciprocal reflectance spectrum of ponds studied. Legend: Chl: maximal absorption by all chlorophyll (isoforms) present, Car: maximal absorption by carotenoids and PC: maximal absorption by phycocyanin. A: The position of minimum absorption by chlorophyll *a*, inorganic suspended matter and water; B: minimal absorption by phytoplankton pigments; Chl *a*: maximal absorption by chlorophyll *a*.

characteristics of the water bodies studied. While the large range of the optically active constituents sampled supported the robustness of the model, Dall'Olmo and Gitelson (2005) suggested that the results should be considered valid only for the ranges of optically active constituents studied (chl *a* range 4.4–217.3 mg/m^3, chl *a* median = 36 mg/m^3; turbidity range 1.7–78 NTU, turbidity median = 17 NTU).

Many water bodies are considered eutrophic to hyper-eutrophic, particularly systems receiving excessive nutrient loadings. One extreme case is represented by aquaculture systems–such as channel catfish production systems–where nutrient daily additions in the form of unassimilated feed can exceed 1.5 mg/l nitrogen addition. In these systems, average chl *a* exceeds 100 mg/m^3 annually and exceeds 700 mg/m^3 during blooms (Tucker, 1996). Windrowing of buoyant algae can increase chl *a* concentrations to more than 10,000 mg/m^3 and turbidity commonly exceeds 140 NTU in these systems (Zimba, unpublished). Clearly hyper-eutrophic systems are not limited to aquaculture ponds, as exemplified by levels of chlorophyll *a* in excess of 9000 μg/l reported from

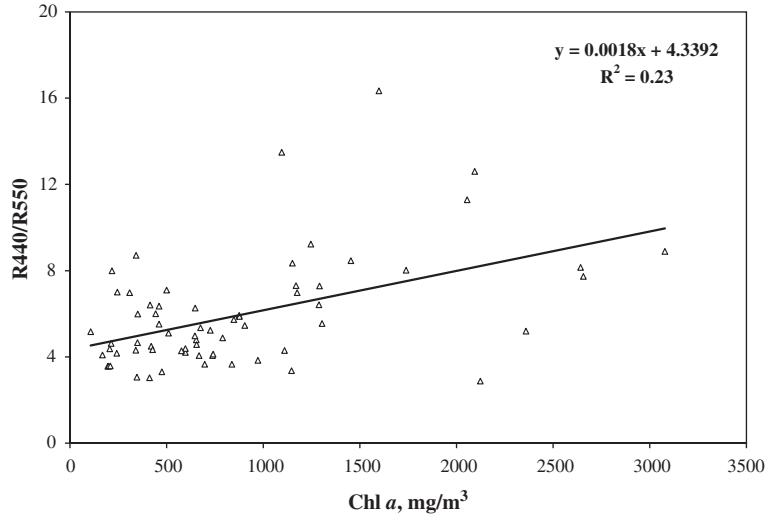

Fig. 4. Relationship between blue to green ratio and measured chlorophyll *a* concentration. Determination coefficient for linear relationship $r^2 = 0.23$. The result shows that blue to green ratio could not be used to estimate chlorophyll *a* concentration in waters studied.

Microcystis blooms in the Patos Lagoon, Brazil (Yunes et al., 1996). These systems are very different from mesotrophic–eutrophic waters routinely studied by remote sensing, where chl *a* and inorganic suspended matter concentrations are much lower.

The main objective of this study was to assess the utility of the conceptual model (Gitelson et al., 2003b; Dall'Olmo and Gitelson, 2005) for estimating chl *a* under high turbidity and algal biomass conditions. Specific objectives include (1) identification of the spectral features of reflectance; (2) spectral tuning of the three band model and the near infrared to red ratio (special case of the three band model) in accord with optical characteristics of the waters studied; and (3) estimating the accuracy of chl *a* retrieval using different algorithms.

2. Methods

Field studies were conducted at the National Warmwater Aquaculture Center, Stoneville, MS using 14–0.4 ha earthen production ponds having an average depth of 0.9 m. Ponds were stocked with channel catfish fry in late May and the average feeding rate was 50 kg/ha of pelleted feed (32% protein). Ponds were managed as commercial operations regarding stocking densities and daily aeration monitoring. Reflectance measurements and water samples were collected weekly from 27 July through 19 September 2004. To assess spatial and temporal variation of chl *a* and reflectance, two additional collections were made in April and May 2005.

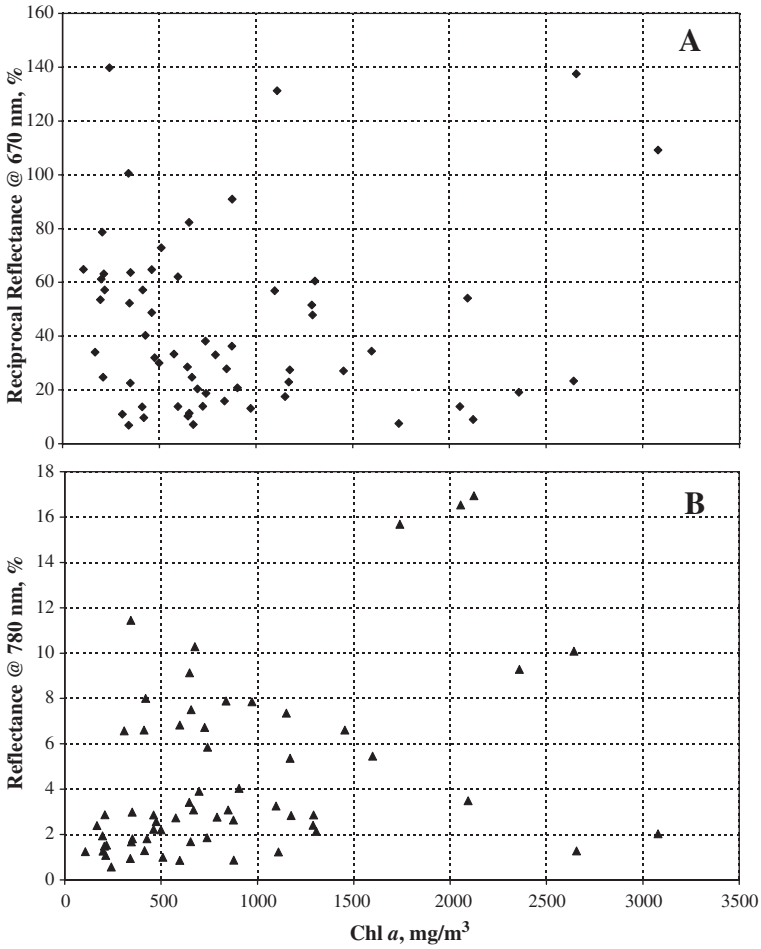

Fig. 5. (A) Reciprocal reflectance at 670 nm vs. chlorophyll *a* concentrations measured analytically. Reciprocal reflectance in the red chlorophyll *a* absorption band depends only weakly on chlorophyll *a* concentrations, suggesting that in addition to chlorophyll *a* reflectance in this spectral range was strongly affected by absorption and scattering of other optically active constituents (e.g., inorganic suspended matter). (B) Reflectance in the near infrared (NIR) range at 780 nm plotted vs. chlorophyll *a* concentration. Concentrations of inorganic suspended matter and phytoplankton density are poorly related, resulting in scattering of R_{780} vs. chlorophyll *a* relationship.

2.1. Field sampling

Water samples and reflectance measurements were collected between 1000 and 1200 h local time. Water samples (1 l volume) were collected immediately after reflectance measurements using tubing attached to a shoreline boom and required < 30 s for sample collection. Sampling depth was 2.5 cm. Water samples were stored in a darkened cooler until processed. Storage time never exceeded 30 min.

A dual-fiber system, with two inter-calibrated Ocean Optics USB2000 radiometers, was used to collect reflectance data in the range 300–850 nm with a sampling interval of 0.3 nm and a spectral resolution of around 1.5 nm. Radiometer 1, equipped with a 25° field-of-view optical fiber, was pointed downward to measure the upwelling radiance of water (L_{up}). Radiometer 2, equipped with an optical fiber and cosine diffuser (yielding a hemispherical field of view), was pointed upward to simultaneously measure incident irradiance (E_{inc}). Downwelling radiance was measured by mounting the optical fiber to a shoreline boom (3 m length). Readings of upwelling radiance were taken with the probe submerged at a fixed depth (2.5 cm) in each pond. To match the transfer functions of the radiometers, intercalibration of the radiometers was accomplished by measuring the upwelling radiance (L_{cal}) of a white Spectralon reflectance standard (Labsphere, Inc., North Sutton, NH) simultaneously with incident irradiance (E_{cal}) measured by upward sensor. Percentage reflectance was computed as:

$$R(\lambda) = [L(\lambda)_{up}/E(\lambda)_{inc}] \times [E(\lambda)_{cal}/L(\lambda)_{cal}] \times 100 \times R(\lambda)_{cal} \quad (2)$$

where $R(\lambda)_{cal}$ is the reflectance of the Spectralon panel linearly interpolated to match the band centers of each radiometer. Data collection and management were

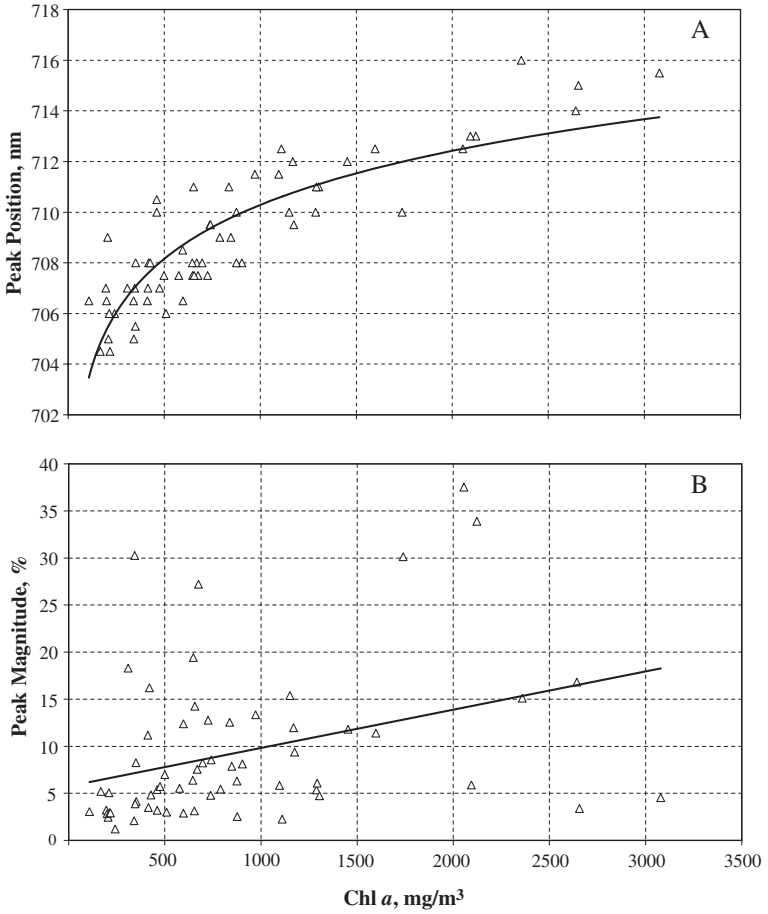

Fig. 6. Position (A) and the magnitude (B) of the peak near 700 nm vs. chlorophyll *a* concentrations. While peak position relates closely to chlorophyll *a* concentration, peak magnitude relates weakly to chlorophyll *a*. It shows that, in addition to chlorophyll *a* absorption, scattering by inorganic and non-living organic suspended matter plays significant role controlling reflectance in this spectral region.

performed using CDAP (a data management program written by CALMIT, University of Nebraska-Lincoln).

The critical issue with regard to the dual-fiber approach is that the transfer functions of both radiometers must be identical. Previous work, using the same instrument configuration, has confirmed that the coefficient of variation of the ratio of the transfer functions of two radiometers does not exceed 0.4% (Dall'Olmo and Gitelson, 2005).

To assess spatial variation of reflectance and chl *a* within a single pond, we measured reflectance and collected five water samples at 1-m intervals along one pond edge. To account for temporal variation of these characteristics, pond location was fixed and five reflectance measurements and water samples were collected at 5-min intervals. Wind speed on both days was less than 0.5 km h^{-1}.

2.2. Laboratory analyses

Water samples were processed under subdued lighting. Turbidity was measured on whole water samples using APHA methodology (APHA, 1989). Chlorophyll and carotenoid concentrations were determined using HPLC methodology as described in Zimba et al. (1999).

3. Results and discussion

The data set encompasses widely variable optical conditions of shallow-water holomictic ponds that exhibit a typical subtropical succession pattern of phytoplankton (Cichra et al., 1995; Tucker, 1996). The waters under study contained chl *a* concentrations of 107 to 3078 mg/m^3 and turbidity from 11 to 423 NTU. Centric diatoms were dominant in spring (April–May); in late spring–early summer (June–July), cryptophytes as well as Oocystaceae (primarily *Chlorella*, *Tetraedon* and *Selenastrum*) and Scenedesmaceae (*Scendesmus*, *Crucigiena* and *Tetradesmus*) green algae were dominant bloom constituents. Summer algae consisted of cyanobacteria (particularly *Dactylococcopsis*, *Oscillatoria*, *Planktothrix* and *Microcystis* spp.—including *M. weisenbergii* and *M. aeruginosa*). Cyanobacteria are dominant constituents of these aquaculture ponds during half of the year (Tucker, 1996; Zimba et al., 2002).

Chl *a* concentration and turbidity (the latter is a proxy of scattering by phytoplankton and inorganic suspended matter) were not related (Fig. 1, determination coefficient of linear relationship <0.05). Clearly chl *a* was not the only characteristic controlling water optical properties, indicating these ponds belong to case 2 waters (Morel and Prieur, 1977).

3.1. Reflectance spectral properties

Reflectance spectra were highly variable over the visible and NIR spectral regions (Fig. 2). These spectra were very different in magnitude from typical reflectance spectra collected in turbid productive waters (Lee et al., 1994; Gitelson et al., 2000; Dall'Olmo and Gitelson, 2005). While reflectance in the blue range was small and did not exceed 5%, green reflectance was very high, reaching 25%, and the peak around 700 nm was even higher, exceeding 30%. Near infrared (NIR) reflectance was also very high and variable (2–18%).

Although reflectance spectra were different in magnitude from those studied previously, the shape of spectra and spectral features were quite similar to that of other productive turbid waters (e.g., Gitelson et al., 2000). In the blue spectral range between 400 and 500 nm, chl *a* and carotenoids strongly absorb light (Fig. 3). The minimum near 440 nm was almost

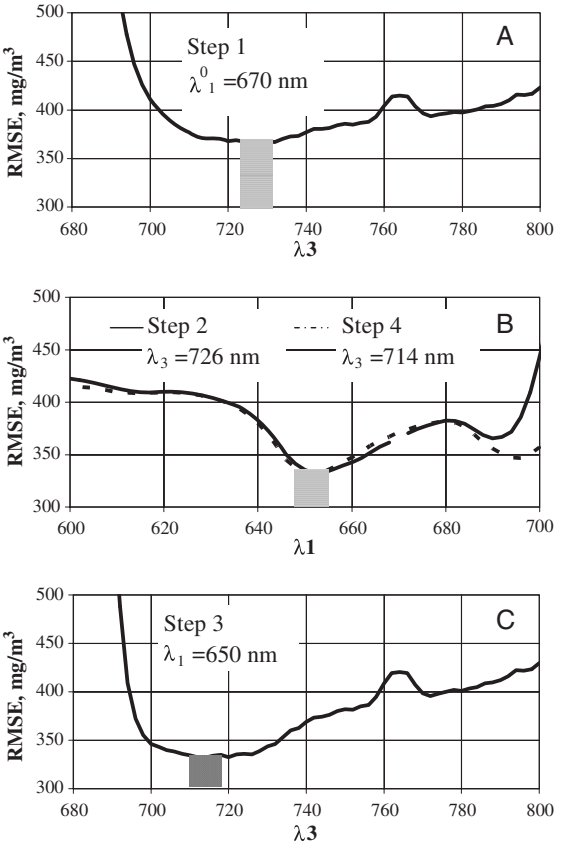

Fig. 7. Four steps of two-band model tuning. Root mean square error of chlorophyll *a* estimation was calculated for linear regression between the model $R(\lambda_3)/R(\lambda_1)$ and chlorophyll *a* concentrations measured analytically.

indistinct in the reflectance spectra and the reflectance in the range 400 to 500 nm was low with no pronounced spectral features over the broad range of turbidity and phytoplankton densities (Fig. 2). Absorption by dissolved organic matter, tripton and scattering by particulate matter contribute to reflectance in the range 400 to 500 nm, and a common characteristic of reflectance spectra in this range was low sensitivity of reflectance to chl *a*. As a result, the blue to green ratio R_{440}/R_{550} (Gordon and Morel, 1983) was not related with chl *a* (Fig. 4) and could not be used to estimate chl *a* in waters studied.

Reciprocal reflectance

$$R^{-1} \propto (a + b_b)/b_b \quad (3)$$

where a and b_b are absorption and backscattering coefficients, respectively, showed several distinct features: (1) a trough in the green range near 550–570 nm (B in Fig. 3) due to the minimal absorption of all algal pigments; scattering by inorganic suspended matter and phytoplankton cells control the magnitude of reflectance in this range; (2) a peak near 625 nm due to phycocyanin absorption (PC in Fig. 3) that typically covaries with cyanobacterial abundance and seasonality (Schalles et al., 1998); (3) a peak at 670–680 nm corresponding to the in situ red chl *a* absorption maximum (chl *a* in Fig. 3); and (4) a minimum in the red/NIR edge near 700 nm (A in Fig. 3).

The magnitude of the reciprocal reflectance peak at 670 nm was poorly correlated with chl *a* concentration as evidenced by the widely scattered data (Fig. 5A). Previous studies have shown that in addition to chl *a* concentration, reflectance in this range was strongly affected by non-organic suspended matter concentration (Gitelson et al., 1993a,b, 1994b, 2000; Dekker, 1993; Yacobi et al., 1995). The effect of chl *a* absorption on reflectance is reduced by light-scattering from phytoplankton cell walls and inorganic suspended matter; the concentrations of these constituents are poorly co-related.

Reciprocal reflectance had a prominent trough around 700 nm (A in Fig. 3) corresponding to a peak in the reflectance spectrum (Fig. 2). In this spectral range, chl *a* absorption decreases with wavelength while absorption by pure water increases. Thus, the trough manifests minimal combined absorption by all constituents (Gitelson et al., 1986, 1993a,b; Vos et al., 1986; Gitelson, 1992). As in other productive turbid waters, the reflectance peak position shifts toward longer wavelengths with increasing chl *a* concentration. Chl *a* has significant absorption between 690 and 715 nm; as chl *a* increases, the absorption curve becomes wider and the intersection point of absorption by chl *a* and pure water takes place at progressively longer wavelengths. Due to the sharp increase in pure water absorption around 710 nm, the relationship between peak position and chl *a* tends to saturate around 715 nm (Fig. 6A). The magnitude of the peak is related to chl *a* concentration, as phytoplankton biomass goes up scattering increases (actually cell surface area to which chl *a* serves as a proxy measure—see Gitelson, 1992, 1993; Gitelson et al., 1994a; Yacobi et al.,

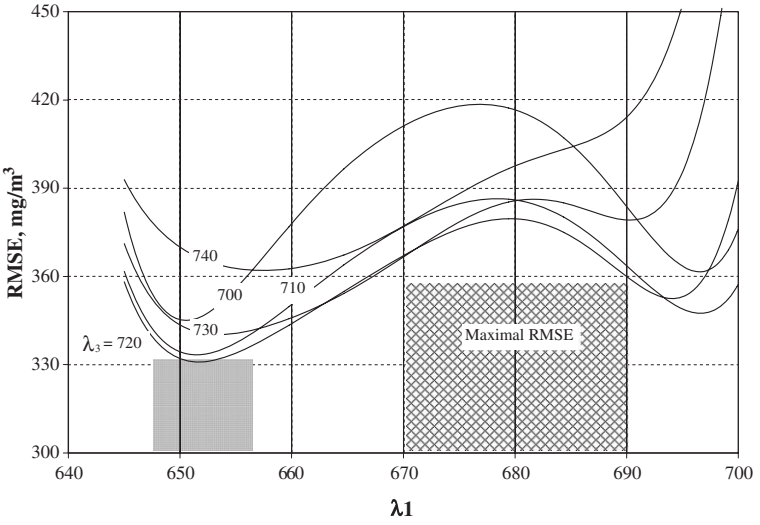

Fig. 8. Root mean square error of chlorophyll *a* estimation by the model $R(\lambda_3)/R(\lambda_1)$ plotted vs. λ_1 for various λ_3. Maximal uncertainties in chlorophyll *a* estimation were found in the range of red chlorophyll *a* absorption around 670 nm and chlorophyll *a* fluorescence at 685 nm. Minimal uncertainties in chlorophyll *a* estimation were around 650 nm (grey box).

1995; Schalles et al., 1998). However, in these waters, chl *a* was responsible for only 11% variation in peak magnitude (Fig. 6B). Scattering by inorganic and non-living organic suspended matter played a critical (if not dominant) role controlling reflectance in this spectral region.

As absorption by all constituents decreases beyond 715–720 nm, the reflectance in the NIR range (R_{NIR}) is controlled by scattering of all particulate matter. Concentrations of inorganic suspended matter and phytoplankton density are poorly related, as indicated by the weak R_{NIR} vs. chl *a* relationship (Fig. 5B).

While the reflectance in the range of chl *a* red absorption around 670 nm is sensitive to chl *a* concentration, it is also affected by absorption and scattering of other constituents. Thus, to accurately retrieve chl *a* from reflectance data, it is critical to subtract the effects of other factors on reflectance around 670 nm. To remove these factors, we used an approach previously used in mesotrophic and eutrophic waters (Dall'Olmo et al., 2003; Dall'Olmo and Gitelson, 2005). In order to find optimal positions of λ_1, λ_2 and λ_3, in the conceptual model (Eq. (1)), we attempted to tune the model and its special case, the band ratio $R(\lambda_3)/R(\lambda_1)$, in accord with optical properties of the medium.

3.2. Two-band ratio model tuning

The two-band model $R(\lambda_3)/R(\lambda_1)$ is the special case of the conceptual model (Eq. (1)) when $a_{chl} \gg b_b$ and $a_{chl} \gg a_{tripton} + a_{CDOM}$, where a_{chl}, $a_{tripton}$ and a_{CDOM} are absorption coefficients of chl *a*, tripton and colored dissolved organic matter (CDOM), respectively (Dall'Olmo and Gitelson, 2005). To find the optimized spectral bands λ_1 and λ_3, we used a stepwise technique based on linear regressions of the $R(\lambda_3)/R(\lambda_1)$ vs. chl *a* measured analytically. For the first step of the model tuning, we used initial position of $\lambda_1^0 = 670$ nm (chl *a* absorption maximum) and linearly regressed the ratio $R(\lambda_3)/R(670)$ vs. chl *a* for each value of λ_3 in the range 400–800 nm. We computed the root mean squared error (RMSE) of chl *a* estimation and found a wide spectral range (between 715 and 730 nm) where RMSE was minimal (Fig. 7A). We selected $\lambda_3^1 = 726^1$nm for the second step of tuning.

In the second step, we regressed the ratio $R(726)/R(\lambda_1)$ vs. chl *a* for each λ_1 in the range 600 to 700 nm. The RMSE had a minimum around 650 nm (Fig. 7B, step 2). We selected $\lambda_1^1 = 650$ nm. In the third step, we found the next approximation of λ_3 regressing the ratio $R(\lambda_3)/R(650)$ vs. chl *a*. The minimal RMSE was found at $\lambda_3^2 = 714$ nm (Fig. 7C). In the last step, we assessed whether $\lambda_1^1 = 650$ nm that we selected in step 2 was optimal. We regressed the ratio $R(714)/R(\lambda_1)$ vs. chl *a* and have found that the optimal λ_1 was very close to $\lambda_1^1 = 650$ nm (Fig. 7B, step 4: dashed line). By using the ratio $R(714)/R(650)$, the error of chl *a* estimation (RMSE = 331 mg/m^3) was minimized.

The plot of RMSE vs. λ_1 for variable λ_3 shows two spectral ranges of λ_1 where RMSE is minimal: (1) around 650 nm for λ_3 in the range from 700 to 730 nm

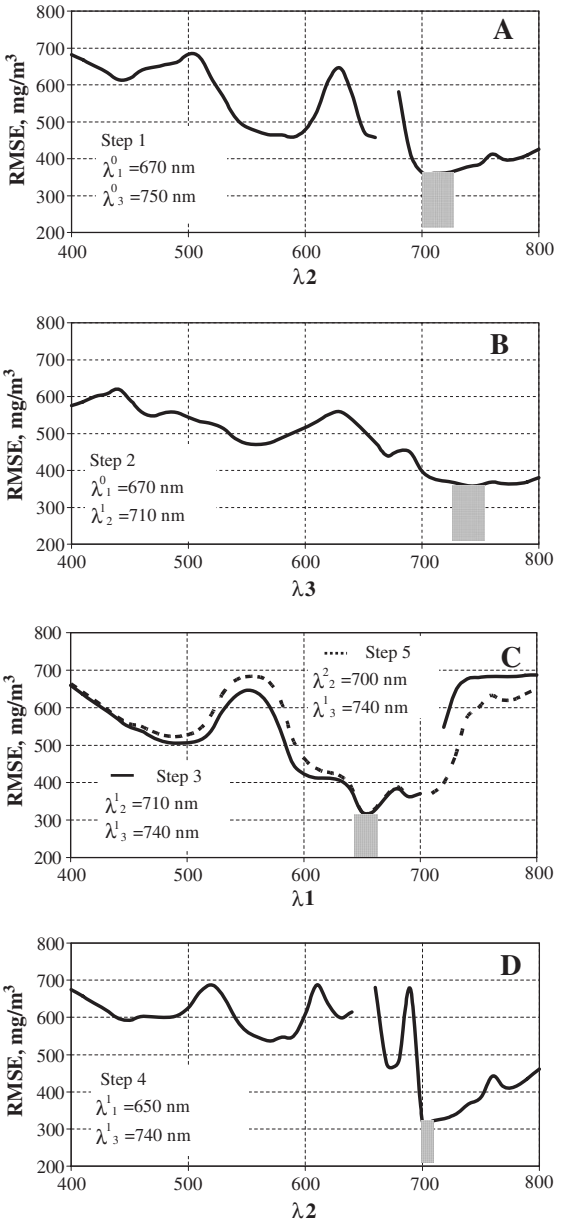

Fig. 9. Five steps of three-band model tuning. RMSE of chlorophyll *a* estimation was calculated for linear regression between the model $[R^{-1}(\lambda_1) - R^{-1}(\lambda_2)] \times R(\lambda_3)$ and chlorophyll *a* concentrations measured analytically.

and (2) 690–695 nm for λ_3 in the range from 700 to 720 nm (Fig. 8). Maximal uncertainties in chl *a* estimation occur in the range between 670 and 690 nm as previously recognized by Dall'Olmo and Gitelson (2005). They concluded that variability in specific absorption coefficient of chl *a* and quantum yield of fluorescence resulted in maximal uncertainties in chl *a* retrieval in the range of chl *a* red absorption (around 670 nm) and chl *a* fluorescence (685 nm).

3.3. Three-band model tuning

To find the first approximation for position of λ_2 (λ_2^1), we used initial positions for $\lambda_1^0=675$ and $\lambda_3^0=750$ nm. The former was chosen within the range of maximum chl *a* absorption, the latter was in the NIR range where scattering controls reflectance. We regressed the model $[R^{-1}(675)-R^{-1}(\lambda_2)]\times R(750)$ vs. chl *a* in the range 400 to 800 nm and found the range between 700 and 720 nm where the RMSE was minimal (Fig. 9A). In the second step, we fixed $\lambda_2^1=710$ nm and regressed the model $[R^{-1}(675)-R^{-1}(710)]\times R(\lambda_3)$ vs. chl *a*. The RMSE was minimal at $\lambda_3^1=740$ nm (Fig. 9B). In the third step, we found the first approximation of $\lambda_1(\lambda_1^1)$, regressing the model $[R^{-1}(\lambda_1)-R^{-1}(710)]\times R(740)$ vs. chl *a*. As in the case of the two-band model (Fig. 7B), the RMSE was minimal in a narrow range around 650 nm (Fig. 9C, solid line). The second approximation of λ_2 (λ_2^2) was found at a slightly shorter wavelength than λ_2^1, in a range between 700 and 715 nm (Fig. 9D). In the final (fifth) step, we verified whether λ_1^1 was optimal, fixing $\lambda_2^2=710$ nm and $\lambda_3^1=740$ nm, and we found that $\lambda_1^1=650$ nm was really optimal wavelength for our data set (Fig. 9C, dash line). Thus, minimal RMSE could be achieved using the model $[R^{-1}(650)-R^{-1}(710)]\times R(740)$.

In the conceptual model, $R^{-1}(\lambda_2)$ is used to account for variations in the a_{tripton} and a_{CDOM} and in b_b (in numerator of Eq. (3)), whereas $R^{-1}(\lambda_3)$ is used to account for variations in b_b (in the denominator of Eq. (3)). Dall'Olmo and Gitelson (2005) reported that the optimal spectral regions for λ_2 and λ_3 overlapped between 730 and 750 nm. The effect of the variability in the backscattering coefficient on reflectance was greater than the variability of tripton and dissolved organic matter absorption. By contrast, our data showed that optimal λ_2 was within a narrow range around 710 nm, while λ_3 was around 740 nm. We hypothesize that in these waters the variability in tripton and dissolved organic matter concentrations was a significant factor and, thus, λ_2 in a narrow range should be used to account for the effect of these constituents. To verify this hypothesis, further study of dissolved organic matter and tripton absorption in these waters is needed.

We evaluated the performance of both the two-band model and the three-band model by comparing their respective root mean square error (RMSE) of chl *a* estimation. Fig. 10 shows relationships between the models, $R(740)/R(710)$ and $[R^{-1}(650)-R^{-1}(710)]\times R(740)$, and chl *a* measured analytically. It can be seen that subtraction $R(740)/R(710)$ from $R(740)/R(650)$

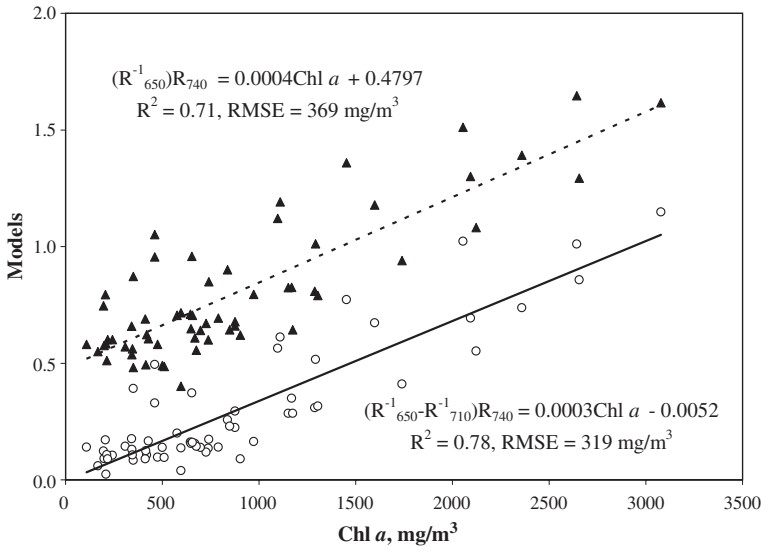

Fig. 10. Two-band model (dash line) and three-band model (solid line) plotted vs. analytically measured chlorophyll *a* concentrations. Subtraction of the $R(\lambda_3)/R(\lambda_2)$ from $R(\lambda_3)/R(\lambda_1)$ improved chlorophyll *a* estimation and made the model $[R^{-1}(\lambda_1)-R^{-1}(\lambda_2)]\times R(\lambda_3)$ proportional to chlorophyll *a* (note that intercept of best fit function of the relationship $[R_{650}^{-1}-R_{710}^{-1}]\times R_{740}$ vs. chlorophyll *a* is very close to zero).

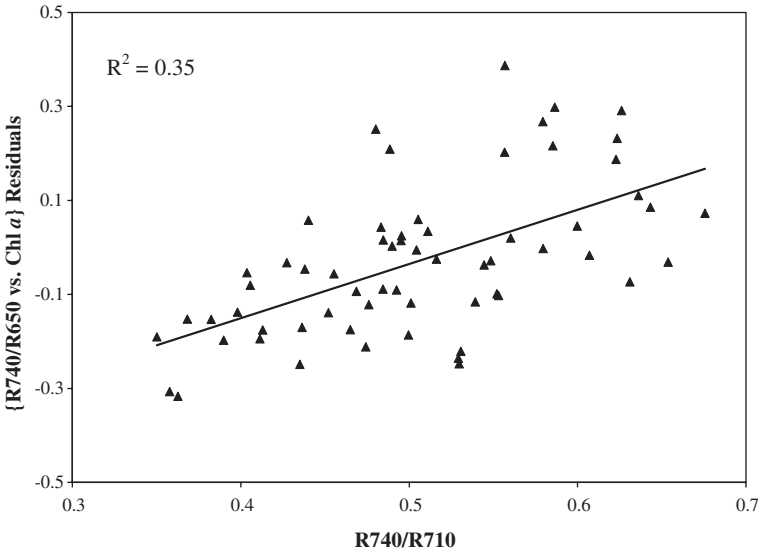

Fig. 11. Residuals of the relationship between R_{740}/R_{650} and chlorophyll *a* (Fig. 10) vs. R_{740}/R_{710}. The ratio R_{740}/R_{710} accounts for more than 34% of variation in residuals. It shows that the subtraction of the R_{740}/R_{710} from R_{740}/R_{650} decreases uncertainties in chlorophyll *a* retrieval due to variability in scattering by particulate matter between samples and in absorption by all constituents, but chlorophyll *a*.

substantially decreases uncertainties in chl *a* retrieval (from 369 to 319 mg/m^3) and makes the intercept of the relationship $[R^{-1}(650)-R^{-1}(710)]\times R(740)$ vs. chl *a* very close to zero. Subtraction is effective in decreasing uncertainties, as evidenced by a statistically significant ($p<0.0001$) positive relationship between the ratio $R(740)/R(710)$ and residuals of the relationship $R(740)/R(650)$ vs. chl *a* (Fig. 11). The ratio $R(740)/R(710)$ accounts for more than 34% of variation in the residuals. Thus, the subtraction of $R(740)/R(710)$ from $R(740)/R(650)$ decreases uncertainties in chl *a* retrieval caused by the variability in scattering by particulate matter between samples and in absorption by constituents other than chl *a*. The comparison of band ratio and three band model performance clearly demonstrated that the latter is more accurate in chl *a* estimation (319 mg/m^3 vs. 330 mg/m^3) and the optimal positions of λ_1 for both models remain around 650 nm (Fig. 12).

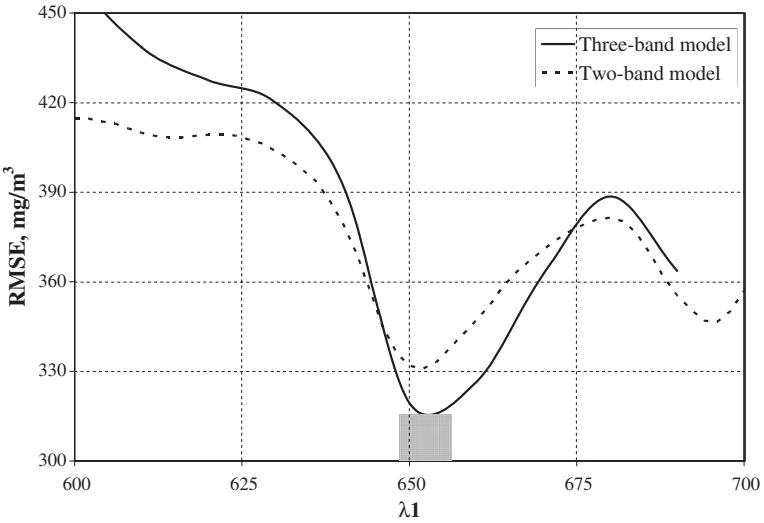

Fig. 12. Root mean square error (RMSE) of chlorophyll *a* estimate by two-band model and three-band model plotted vs. λ_1. While the optimal positions of λ_1 for both models remain almost the same (around 650 nm), the three-band model is more accurate in chlorophyll *a* estimation (319 mg/m^3 vs. 330 mg/m^3).

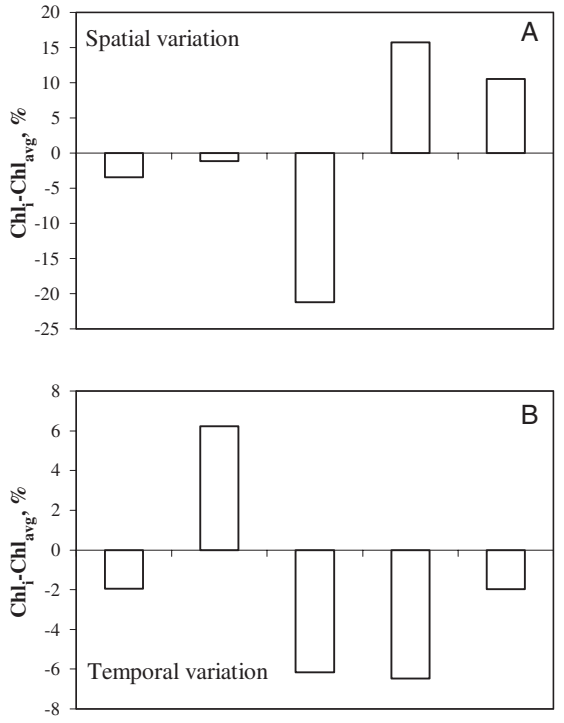

Fig. 13. Spatial (A) and temporal (B) variation (%) of chlorophyll *a* concentrations from mean values (number of samples $n=5$ each). Coefficient of variation was 14% (spatial) and 7.4% (temporal).

The band ratio model explains 71% and three-band model 78% of chl *a* variability (Fig. 10). It is likely that phytoplankton patchiness was partially responsible for unexplained chl *a* variation. Both spatial and temporal wind driven circulation strongly influences phytoplankton patchiness in lakes (Small, 1963; Reynolds, 1971; Verhagen, 1994), particularly in shallow systems (Cichra et al., 1995). To assess the importance of this factor, we plotted spatial (Fig. 13A) and temporal (Fig. 13B) variation of chl *a* (in percent) from mean values in five samples for each case. Spatial variability exceeded ± 15%, while temporal variation exceeded ± 6%. Temporal and spatial variability of reflectance was even higher: the coefficient of spatial variation reached 30% and temporal variation was higher than 60% (Fig. 14). Similar findings were reported in Yacobi et al. (1995) assessing Lake Kinneret's seasonal *Protoperidium* blooms. In the Lake Kinneret study, up to 300% difference in reflectance and chl *a* was reported at 10-m intervals (spatial) and in samples collected at 2.5-min intervals (temporal) from one sampling site.

The findings point out the need for optimal simultaneous collection of ground-truth samples and reflectance to accurately calibrate the models for chl *a* assessment in these dynamic systems. It also shows that data used as "ground-truth" can vary significantly in time and space and might not represent constituent concentrations when and where reflectance was measured. Even when ground-truth samples are collected simultaneously with reflectance data, the sampling procedure (physical manipulation of water column) can significantly change constituent concentrations resulting in poor correlations with to concurrent reflectance spectra measured remotely.

Previous studies that used generalized models and did not take into account the impact of temporal variation or spatial patchiness poorly predicted chl *a* concentration from reflectance data (Zimba and Thomson, 2002; Millie et al., 1995). It is therefore not surprising that empirical models derived from simultaneously measured "ground-

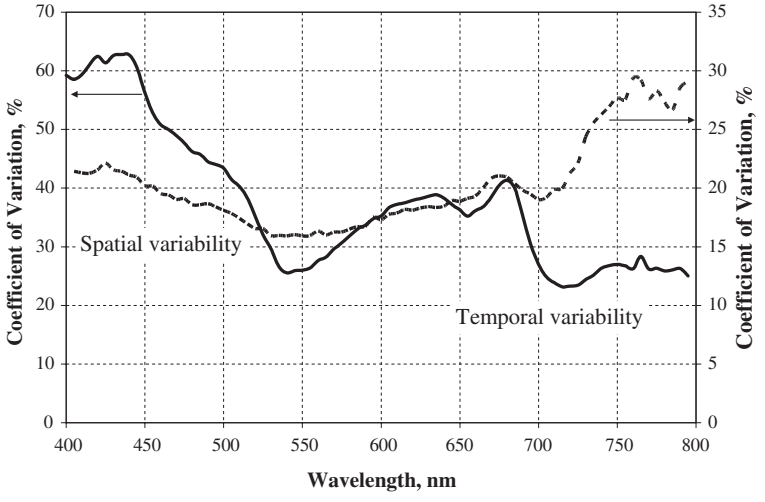

Fig. 14. Temporal and spatial variation of reflectance spectra of the ponds. Coefficient of temporal variation was above 20% and coefficient of spatial variation was above 15%.

truth data" and aerial overflights were unable to fit data collected 1 month later (Millie et al., 1995) and that predicted chl *a* and measured values were poorly correlated ($R^2=0.4$, Zimba and Thomson, 2002). Choice of appropriate scales for (multi-dimensional) field assessments must consider sample size (reviewed in Cassie, 1959), location (McAlice, 1970) and time (this study; Yacobi et al., 1995). Sampling surface blooms of buoyant microalgae (such as *Microcystis*) further complicate sample collection, as any surface disturbance influence cell distributions. Optimal management of water resources will depend on both generation of optimal physically based models to quantify algal biomass and improved sampling methods to calibrate it.

It is noteworthy that the three-band model ($\lambda_1=670$ nm, $\lambda_2=710$ nm, $\lambda_3=740$ nm) optimized for chl *a* ranging from 4.4 to 217.3 mg/m^3 (Dall'Olmo and Gitelson, 2005) allowed accurate estimation of chl *a* when applied to these aquaculture ponds having very different optical characteristics, and it allowed accurate chl *a* estimation with RMSE below 358 mg/m^3. Thus, the model with fixed spectral bands works accurately in the range of chl *a* from 4.4 to 3078 mg/m^3 allowing monitoring of chl *a* in waters with low-to-moderate chl *a* concentrations as well as extremely turbid and hyper-eutrophic waters.

The models used in this study do not require data on bio-optical characteristics of the waters—these can be variable and difficult to obtain. Instead, tuning spectral band positions of the model minimized the effect of variability in bio-optical parameters and increased the model accuracy. Additionally, the cost associated with hand-held units and ease of use offer widespread application in specialized environments such as aquaculture systems.

The conceptual model (Eq. (1)) has been used for non-destructive pigment retrieval from reflectance spectra of plant leaves (anthocyanins: Gitelson et al., 2001; carotenoids: Gitelson et al., 2002; chlorophyll: Gitelson et al., 2003a), fruit peels (Merzlyak et al., 2003), crop canopies (Gitelson et al., 2003b, 2005) and chl *a* retrieval in turbid productive waters (Dall'Olmo et al., 2003; Dall'Olmo and Gitelson, 2005, in press). This study brings additional evidence that the conceptual model may be considered as a unified approach for remote quantification of absorbing constituents in variety of systems.

Acknowledgements

Mention of a trade name, proprietary product or specific equipment does not constitute a guarantee or warranty by the US Department of Agriculture and does not imply approval of the product to the exclusion of other products that may be available. This research was supported partially by the Grant to AG from USDA/ARS/MSA No. SCA 58-6402-4-075. We greatly acknowledge G. Keydan (UNL) for assistance in data processing and field assistance by S. Towery, M. Fuller, and W. Jobe. A contribution of the University of Nebraska Agricultural Research Division, Lincoln, NE, Journal Series No. 15141. This research was also supported in part by funds provided through the Hatch Act.

References

APHA, 1989. American Water Works Association, and Water Pollution Control Federation. Standard Methods for the Examination of Water and Wastewater. American Public Health Association, Washington, D.C.

Australian Government Department of the Environment and Heritage website http://www.deh.gov.au/water/rivers/nrhp/.

Bricaud, A., Babin, M., Morel, A., Claustre, H., 1995. Variability in the chlorophyll-specific absorption coefficients of natural phytoplankton: analysis and parameterization. J. Geophys. Res. [Oceans] 100, 13321–13322.

Cassie, R.M., 1959. Microdistribution of plankton. In: Barnes, H. (Ed.), Oceanogr. Mar. Biol. Ann. Rev., vol. 1, pp. 223–252.

Cichra, M.F., Badylak, S., Henderson, N., Ruetter, B.H., Phlips, E.J., 1995. Phytoplankton community structure in the open water zone of a shallow subtropical lake (Lake Okeechobee, Florida, USA). Archiv. Hydrobiol. Spec. Issues Advanc. Limnol. 45, 157–175.

Dall'Olmo, G., Gitelson, A.A., 2005. Effect of bio-optical parameter variability on the remote estimation of chlorophyll-*a* concentration in turbid productive waters: experimental results. Appl. Opt. 44, 412–422.

Dall'Olmo, G., Gitelson, A.A., in press. Effect of bio-optical parameter variability and uncertainties in reflectance measurements on the remote estimation of chlorophyll-*a* concentration in turbid productive waters: modeling results. Applied Optics, Posted at Applied Optics web: 12 December 2005.

Dall'Olmo, G., Gitelson, A.A., Rundquist, D.C., 2003. Towards a unified approach for remote estimation of chlorophyll-*a* in both terrestrial vegetation and turbid productive waters. Geophys. Res. Lett. 30, 1038. doi:10.1029/2003GL018065.

Dall'Olmo, G., Gitelson, A.A., Rundquist, D.C., Leavitt, B., Barrow, T., Holz, J.C., 2005. Assessing the potential of SeaWiFS and MODIS for estimating chlorophyll concentration in turbid productive waters using red and near-infrared bands. Remote Sens. Environ. 96, 176–187.

Dekker, A., 1993. Detection of the optical water quality parameters for eutrophic waters by high resolution remote sensing. Ph.D. Thesis, Free University, Amsterdam, The Netherlands. 212 pp.

Doerffer, R., 1981. Factor analysis in ocean color interpretation. In: Gower, J.F.R. (Ed.), Oceanography from Space. Plenum Press, New York, pp. 339–345.

Fischer, J., Kronfeld, V., 1990. Sun-stimulated chlorophyll fluorescence: 1. Influence of oceanic properties. Int. J. Remote Sens. 11, 2125–2147.

Gitelson, A.A., 1992. The peak near 700 nm on reflectance spectra of algae and water: relationships of its magnitude and position with chlorophyll concentration. Int. J. Remote Sens. 13, 3367–3373.

Gitelson, A., 1993. The nature of the peak near 700 nm on the radiance spectra and its application for remote estimation of phytoplankton pigments in inland waters. Optical Engineering and Remote Sensing, 1971. SPIE, pp. 170–179.

Gitelson, A.A., Kondratyev, K.Y., 1991. Optical models of mesotrophic and eutrophic water bodies. Int. J. Remote Sens. 12, 373–385.

Gitelson, A., Nikanorov, A.M., Sabo, G., Szilagyi, F., 1986. Etude de la qualite des eaux de surface par teledetection. IAHS Publ. 157, 111–121.

Gitelson, A., Garbuzov, G., Szilagyi, F., Mittenzwey, K.-H., Karnieli, A., Kaiser, A., 1993a. Quantitative remote sensing methods for real-time monitoring inland water quality. Int. J. Remote Sens. 14, 1269–1295.

Gitelson, A., Szilagyi, F., Mittenzwey, K., 1993b. Improving quantitative remote sensing for monitoring of inland water quality. Water Res. 7, 1185–1194.

Gitelson, A., Mayo, M., Yacobi, Y.Z., 1994a. Signature analysis of reflectance spectra and its application for remote observations of the phytoplankton distribution in Lake Kinneret. Mesures Physiques et Signatures en Teledetection. ISPRS 6th International Symposium, pp. 277–283.

Gitelson, A., Mayo, M., Yacobi, Y.Z., Parparov, A., Berman, T., 1994b. The use of high spectral radiometer data for detection of low chlorophyll concentrations in Lake Kinneret. J. Plankton Res. 16, 993–1002.

Gitelson, A.A., Yacobi, Y.Z., Schalles, J.F., Rundquist, D.C., Han, L., Stark, R., Etzion, D., 2000. Remote estimation of phytoplankton density in productive waters. Arch. Hydrobiol. Spec. Issues Advanc. Limnol. 55, 121–136.

Gitelson, A.A., Merzlyak, M.N., Chivkunova, O.B., 2001. Optical properties and non-destructive estimation of anthocyanin content in plant leaves. Photochem. Photobiol. 74 (1), 38–45.

Gitelson, A.A., Zur, Y., Chivkunova, O.B., Merzlyak, M.N., 2002. Assessing carotenoid content in plant leaves with reflectance spectroscopy. Photochem. Photobiol. 75 (3), 272–281.

Gitelson, A.A., Gritz, U., Merzlyak, M.N., 2003a. Relationships between leaf chlorophyll content and spectral reflectance and algorithms for non-destructive chlorophyll assessment in higher plant leaves. J. Plant Physiol. 160, 271–282.

Gitelson, A.A., Viña, A., Arkebauer, T.J., Rundquist, D.C., Keydan, G., Leavitt, B., 2003b. Remote estimation of leaf area index and green leaf biomass in maize canopies. Geophys. Res. Lett. 30, 1248. doi:10.1029/2002GL016450.

Gitelson, A.A., Viña, A., Ciganda, V., Rundquist, D.C., Arkebauer, T.J., 2005. Remote estimation of canopy chlorophyll content in crops. Geophys. Res. Lett. 32, L08403. doi:10.1029/2005GL022688.

Gons, H.J., 1999. Optical teledetection of chlorophyll a in turbid inland waters. Environ. Sci. Technol. 33, 1127–1132.

Gons, H.J., Rijkeboer, M., Bagheri, S., Ruddick, K.G., 2000. Optical teledetection of chlorophyll *a* in estuarine and coastal waters. Environ. Sci. Technol. 34, 5189–5192.

Gordon, H., Morel, A., 1983. Remote Assessment of Ocean Color for Interpretation of Satellite Visible Imagery. A Review. Lecture notes on Coastal and Estuarine Studies, vol. 4. Springer-Verlag, New York. 114 pp.

Gower, J.F.R., 1980. Observations of in-situ fluorescence of chlorophyll-*a* in Saanich Inlet. Boundary - Layer Meteorol. 18, 235–245.

Gower, J.F.R., Doerffer, R., Borstad, G.A., 1999. Interpretation of the 685 nm peak in water-leaving radiance spectra in terms of fluorescence, absorption and scattering, and its observation by MERIS. Int. J. Remote Sens. 20, 1771–1786.

GKSS, 1986. The use of chlorophyll fluorescence measurements from space for separating constituents of sea water. ESA Contract No. RFQ3-5059/84/NL/MD, Vol II, Appendices, GKSS, Research Centre, Germany.

Hoge, E.F., Wright, C.W., Swift, R.N., 1987. Radiance ratio algorithm wavelengths for remote oceanic chlorophyll determination. Appl. Opt. 26, 2082–2094.

Lee, Z.P., Carder, K.L., Hawes, S.K., Steward, R.G., Peacock, T.G., Davis, C.O., 1994. Model for the interpretation of hyperspectral remote-sensing reflectance. Appl. Opt. 33, 5721–5732.

Matthews, A.M., Boxall, S.R., 1994. Novel algorithms for the determination of phytoplankton concentration and maturity. Proc. of the Second Thematic Conference on Remote Sensing for Marine and Coastal Environments, vol. 1, pp. 173–180.

McAlice, B.J., 1970. Observations on the small-scale distribution of estuarine phytoplankton. Mar. Biol. 8, 100–111.

Merzlyak, M.N., Solovchenko, A.E., Gitelson, A.A., 2003. Reflectance spectral features and non-destructive estimation of chlorophyll, carotenoid and anthocyanin content in apple fruit. Postharvest Biol. Technol. 27, 197–211.

Millie, D.F., Vinyard, B.T., Baker, M.C., Tucker, C.S., 1995. Testing the temporal and spatial validity of site-specific models derived from airborne remote sensing. Can. J. Fish Aquat. Sci. 52, 1094–1107.

Morel, A., Prieur, L., 1977. Analysis of variations in ocean color. Limnol. Oceanogr. 22, 709–722.

Neville, R.A., Gower, J.F.R., 1977. Passive remote sensing of phytoplankton via chlorophyll *a* fluorescence. J. Geophys. Res. 82, 3487–3493.

Oki, K., Yasuoka, Y., 2002. Estimation of chlorophyll concentration in lakes and in-land seas with a field spectroradiometer above the water surface. Appl. Opt. 41, 6463–6469.

Pierson, D., Sträombäack, N., 2000. A modeling approach to evaluate preliminary remote sensing algorithms: use of water quality data from Swedish great lakes. Geophysica 36, 177–202.

Pulliainen, J., Kallio, K., Eloheimo, S., Koponen, H., Servomaa, T., Hannonen, S., Tauriainen, J., Hallikainen, M., 2001. A semi-operative approach to lake water quality retrieval from remote sensing data. Sci. Total Environ. 268, 79–93.

Quibell, G., 1992. Estimation chlorophyll concentrations using upwelling radiance from different freshwater algal genera. Int. J. Remote Sens. 13, 2611–2621.

Reynolds, C.S., 1971. The ecology of the blue-green algae in the North Shropshire meres. Field Stud. 3, 409–432.

Ruddick, K.G., Gons, H.J., Rijkeboer, M., Tilstone, G., 2001. Optical remote sensing of chlorophyll a in case 2 waters by use of an adaptive two-band algorithm with optimal error properties. Appl. Opt. 40, 3575–3585.

Schalles, J.F., Gitelson, A., Yacobi, Y.Z., Kroenke, A.E., 1998. Chlorophyll estimation using whole seasonal, remotely sensed high spectral-resolution data for an eutrophic lake. J. Phycol. 34, 383–390.

Small, L.F., 1963. Effect of wind on the distribution of chlorophyll *a* in Clear Lake, Iowa. Limnol. Oceanogr. 8, 426–432.

Tucker, C.S., 1996. The ecology of channel catfish culture in northwest Mississippi. Rev. Fish. Sci. 8, 45–88.

Verhagen, J.H.G., 1994. Modeling phytoplankton patchiness under the influence of wind-driven currents in lakes. Limnol. Oceanogr. 39, 1551–1565.

Vitousek, P.M., Mooney, H.A., Lubchenco, J., Melillo, J.M., 1997. Human domination of Earth's ecosystems. Science 277, 494–499.

Vos, W.L., Donze, M., Bueteveld, H., 1986. On the reflectance spectrum of algae in water: the nature of the peak at 700 nm and its shift with

varying concentration. Technical Report. Communication on Sanitary Engineering and water Management, Delft, The Netherlands, p. 86-22.

Yacobi, Y.Z., Gitelson, A., Mayo, M., 1995. Remote sensing of chlorophyll in Lake Kinneret using high spectral resolution radiometer and Landsat TM: spectral features of reflectance and algorithm development. J. Plankton Res. 17, 2155–2173.

Yunes, J.S., Salomon, P.S., Matthiensen, A., Beattie, K.A., Raggett, S.L., Codd, G.A., 1996. Toxic blooms of cyanobacteria in the Patos Lagoon Estuary, southern Brazil. J. Aquat. Ecosyst. Health 5, 223–229.

Zimba, P.V., Thomson, S., 2002. Detection of toxin-producing algae by low altitude remote sensing methods. 7th Int. Conf. Remote Sens. Mar. Coast. Env. Paper, vol. 15, p. 3.

Zimba, P.V., Dionigi, C.P., Millie, D.F., 1999. Evaluating the relationship between photopigment synthesis and 2-methylisoborneol accumulation in cyanobacteria. J. Phycol. 35, 1422–1429.

Zimba, P.V., Mischke, C., Tucker, C.S., Grimm, C.C., 2002. Short-term effects of diuron in catfish production ponds. N. Am. J. Aquac. 64, 16–23.